

An Algorithm for Operating a Fed-Batch Fermentor at Optimum Specific-Growth Rate

Pramod Agrawal,* George Koshy, and Michael Ramseier
*Department of Chemical Engineering, University of California,
Santa Barbara, California 93106*

Accepted for publication December 18, 1987

An algorithm for operating a fed-batch fermentor at an optimum specific fermentation rate is proposed. It does not require on-line measurement of nutrient concentration in the culture medium. An on-line estimate of the specific fermentation rate is sufficient for implementation of this scheme. The algorithm is model independent and works well even with poor estimates of the product yields and the specific fermentation rate. Results of a detailed simulation study are presented for a simple case of optimization of cell-mass production in a fed-batch fermentor. The results clearly demonstrate the efficacy of this algorithm under a wide range of fermentation situations.

INTRODUCTION

Most fermentation processes are operated in either batch or fed-batch mode. Over the past few years, the fed-batch mode¹ has been introduced in an increasing number of fermentation processes. This is because theoretical analysis² of many fermentation processes have revealed the extended or exponentially fed-batch cultures to be optimal. Fed-batch fermentations have also gained popularity because of the improved control possibilities using computer-coupled fermentation systems.^{3,4} Constantinides,⁵ Yamane and Shimizu,⁶ and Parulekar and Lim⁷ have given extensive reviews of the subject on fed-batch fermentation.

In recent years, several reports⁸⁻¹⁰ have appeared on the problem of optimal operation of a fed-batch fermentor with respect to various objective functions and control variables. The most common measure of the performance of these systems is the fermentor's productivity. It is usually optimized by manipulating the nutrient flow rate according to a predetermined program derived using a fermentation model and an optimizing principle.^{1,2} For example, for the case of a microbial system exhibiting substrate-inhibited kinetics, Weigand¹ utilized Pontryagin's maximum principle to derive the optimal feeding strategy to maximize the biomass productivity in a repeated fed-batch fermentor. A common problem⁶ with open loop implementation of an optimal feed

program obtained by such a procedure is that considerable deviations in the state of a fermentor from the optimal state may occur if disturbances enter the system during the fermentation. Two types of feedback-controlled fed-batch fermentations have been introduced⁶ to overcome this problem. These are classified as indirect feedback controlled and direct feedback controlled fed-batch fermentations. A fed-batch operation with indirect feedback control utilizes an observable parameter, such as dissolved oxygen, pH, respiratory quotient, or partial pressure of CO₂, which is closely related to the course of the microbial fermentation. In the second type of feedback-controlled fermentation, the concentration of the limiting substrate in the culture medium is directly utilized as a feedback parameter. Very few reports, however, have appeared on direct feedback controlled fed-batch fermentations. This could be because of the difficulty associated with obtaining accurate on-line measurements of substrate concentrations.

Another major problem with the implementation of a predetermined feed schedule is that the model used to develop the optimum feed schedule be valid under a variety of conditions. This requirement is not met in many fermentation processes where models developed based on steady-state data work only qualitatively under transient conditions. Moreover, strain modification due to microbial adaptation or a change in the quality of nutrient medium could cause large variations in the values of parameters used to model a system. Such changes make an otherwise optimal feed schedule nonoptimal.

The problems discussed above point a need for development of a fed-batch fermentation strategy which is model independent, identifies the optimal state on-line, and incorporates a negative feedback control into the nutrient feeding system. In this paper we present a method for operating a fed-batch fermentor at the maximum possible specific rate of fermentation. This is of importance in a number of fermentation processes where the main objective is to maximize the fermentor productivity. For example, the cell-mass productivity in a fed-batch fermentor is maximized¹ by operating the fermentor under the condition of optimal specific growth rate (μ_{opt}).

* To whom all correspondence should be addressed.

To implement the proposed algorithm, it is not essential to have on-line measurements of nutrient concentrations in the culture medium. It only requires a reliable on-line estimate of the specific-fermentation rate. This article describes the important features of this algorithm and presents the results of a detailed simulation study which demonstrates its efficacy and compares its results to optimal fed-batch fermentation results based on predetermined feed schedules. For convenience, we consider only the problem of optimizing the cell-mass production in a fed-batch fermentor.

MODEL EQUATIONS AND CONDITIONS

The generalized balance equations for conversion of substrate (S) to cell mass (X) and product (P) in a variable-volume fermentor with cell-free and product free feed containing the limiting substrate at a concentration S_F can be written as

$$\frac{dV}{dt} = F_{in} - F_{out} \quad (1)$$

$$\frac{dX}{dt} = -\frac{F_{in}}{V}X + \mu X \quad (2)$$

$$\frac{dS}{dt} = \frac{F_{in}}{V}(S_F - S) - \frac{\mu X}{y_{X/S}} \quad (3)$$

$$\frac{dP}{dt} = -\frac{F_{in}}{V_p} + \pi X \quad (4)$$

where μ is the specific-growth rate; π is the specific product formation rate; and $y_{X/S}$ is the yield of cell mass with respect

to the limiting substrate. The growth models used in the simulation study are listed in Table I along with the parameter values for each model and the feed-substrate concentration values. Model 1 doesn't exhibit an optimum in μ with respect to S , whereas each of the models 2, 3, and 4 exhibits optima at $\mu = \mu_{opt}$ for specific values of $S = S_{opt}$. Moreover, the μ_{opt} values in models 2 and 3 remain constant; whereas, due to the product inhibition term, the μ_{opt} value in model 4 decreases with an increase in the product concentration in the medium. In all fed-batch fermentation simulations, the initial volume (V_0) and the final volume (V_m) are assumed to be 2.0 and 10 L, respectively. The initial substrate concentration (S_0) is assumed to be 0 g/L and the initial cell-mass concentration (X_0) is assumed to be 8.0 g/L. These values roughly correspond to the conditions that exist after a batch run is carried out at an initial substrate concentration equal to the feed-substrate concentration indicated in Table I.

RESULTS AND DISCUSSION

Open-Loop Performance

To demonstrate some of the shortcomings of implementing a predetermined feed schedule to optimize productivity in a fed-batch fermentor, we consider the microbial system *Candida utilis*. This microorganism exhibits the substrate-inhibited kinetics¹¹ as described by Model 2 in Table I. The model exhibits an optimum specific growth rate, μ_{opt} , at a substrate concentration of S_{opt} .

Table I. List of models and associated parameter values.

Model	Form	Parameter values
1) Monod (Saturation kinetic)	$\mu = \frac{\mu_m S}{K_m + S}$	$\mu_m^{-1} = 0.53 \text{ h}^{-1}$ $K_m = 1.2 \text{ (g/L)}$
Constant yield	$y_{X/S} = y_0$	$y_0 = 0.4 \text{ (g/g)}$ $S_F = 20 \text{ (g/L)}$
2) Substrate inhibition	$\mu = \frac{\mu_m S}{K_m + S + S^2/K_i}$	$\mu_m = 0.53\text{--}0.66 \text{ h}^{-1}$ $K_m = 1.2 \text{ (g/L)}$ $K_i = 22 \text{ (g/L)}$
Constant yield	$y_{X/S} = y_0$	$y_0 = 0.3\text{--}0.4 \text{ (g/g)}$ $S_F = 15\text{--}20 \text{ (g/L)}$
3) Substrate inhibition	$\mu = \frac{\mu_m S(1 - aS)}{K_m + S + S^2/K_i}$	$\mu_m = 0.504 \text{ h}^{-1}$ $a = 0.0204 \text{ (g/L)}$ $K_m = 0.00849 \text{ (g/L)}$ $K_i = 24.63 \text{ (g/L)}$
Variable yield ¹²	$y_{X/S} = \frac{y_0(1 - aS)}{1 + bS + cS^2}$	$y_0 = 0.383 \text{ (g/g)}$ $b = 0.296 \text{ (g/L)}^{-1}$ $c = -0.00501 \text{ (g/L)}^{-2}$ $S_F = 20 \text{ (g/L)}$
4) Substrate and product inhibitions	$\mu = \frac{\mu_m S}{K_m + S + S^2/K_i}$ $\mu_m = \mu_m^0 \left(1 - \frac{P}{P_m}\right)$	$\mu_m^0 = 0.48 \text{ h}^{-1}$ $K_m = 1.2 \text{ (g/L)}$ $K_i = 22 \text{ (g/L)}$ $P_m = 50 \text{ (g/L)}$
Constant yields	$\pi = \alpha\mu + \beta$ $\alpha, \beta, \text{ and } y_{P/S}$	$\alpha = 2.2 \text{ (g/g)}$ $\beta = 0.2 \text{ h}^{-1}$ $\theta_{P/S} = 0.88 \text{ (g/g)}$ $S_F = 15 \text{ (g/L)}$

The feed schedule for optimization of cell-mass productivity developed by Weigand¹ using Pontryagin's maximum principle is applicable to the above microbial system. It consists of rapid fill and singular fill stages as shown in Figure 1(a). During rapid fill the nutrients are fed at the maximum rate to quickly raise the limiting substrate concentration to its optimum value, S_{opt} . The singular fill interval then begins, during which substrate is fed at a rate equal to its consumption, such that S and μ are maintained at S_{opt} . When the fermentor volume reaches its maximum value, a batch stage may be initiated in order to meet the terminal substrate condition.

We now examine a case in which one of the model parameters, μ_m , is incorrectly identified. This could occur if the cells exhibit a different value of μ_m due to a change in the culture condition. The true μ_m value is assumed to be 25% higher than the value in the model used to determine the optimum feed policy. Under this situation use of the optimal feed schedule determined based on the incorrect model results in considerable deviation of the specific growth rate from its optimum value as shown in Figure 2(a). This is because the feed profile based on the incorrect model leads to substrate concentrations far below the optimum value resulting in a nonoptimal operation. Similar nonoptimal performance is seen [Fig. 3(a)] in a case where the microbial culture exhibits a cell-mass yield, $y_{X/S}$, which is 25% lower than the value used in the model.

Development and Evaluation of Control Algorithm

The above results show that a model-based, open-loop feed policy does not always result in an optimal operation. To overcome this problem, we propose a feedback control algorithm which only requires a reliable on-line estimate of the specific-growth rate, μ . With the rapid development of computer-coupled fermentation systems, this is not a difficult problem. Wu and co-workers¹³ have successfully used the oxygen uptake rate to obtain good on-line estimates of μ in baker's yeast fermentation. Park and co-workers¹⁴ have used the CO_2 evolution rate for on-line estimation of μ in a glutamic-acid fermentation. Acid-production rate has also been used to provide on-line estimates of μ in baker's yeast fermentation.¹⁵ In this study we assume that on-line estimates of μ are available every two minutes. Since the objective of the algorithm is to optimize the cell-mass production by controlling μ at μ_{opt} , a simple feedback law of the form

$$F_{in}(t_{n+1}) = F_{in}(t_n) \pm K_c [\mu_{opt}(t_n) - \mu(t_n)] \quad (5)$$

could be used to manipulate the feed flow rate (F_{in}) to the fermentor, where K_c in eq. (5) is a controller constant which is assumed to be positive. When $\mu \neq \mu_{opt}$, either $S < S_{opt}$ or $S > S_{opt}$. The positive sign in eq. (5) applies to the former case in which the controller must drive S toward S_{opt} by in-

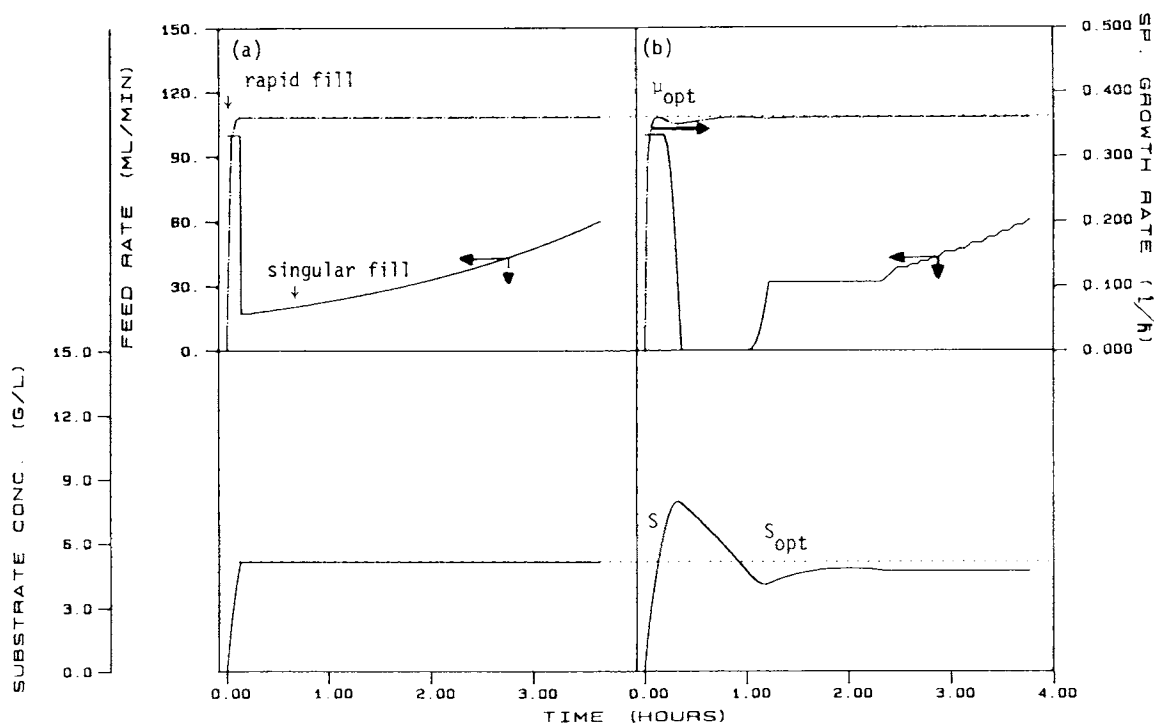


Figure 1. Specific growth rate (—) μ and (·····) μ_{opt} , substrate concentration (—) S and (·····) S_{opt} , and (—) feed-flow rate profiles for (a) optimal open-loop solution for cell-mass productivity based on maximum principle applied to Model 2, and (b) feedback controlled operation ($K_c = 12$ L).

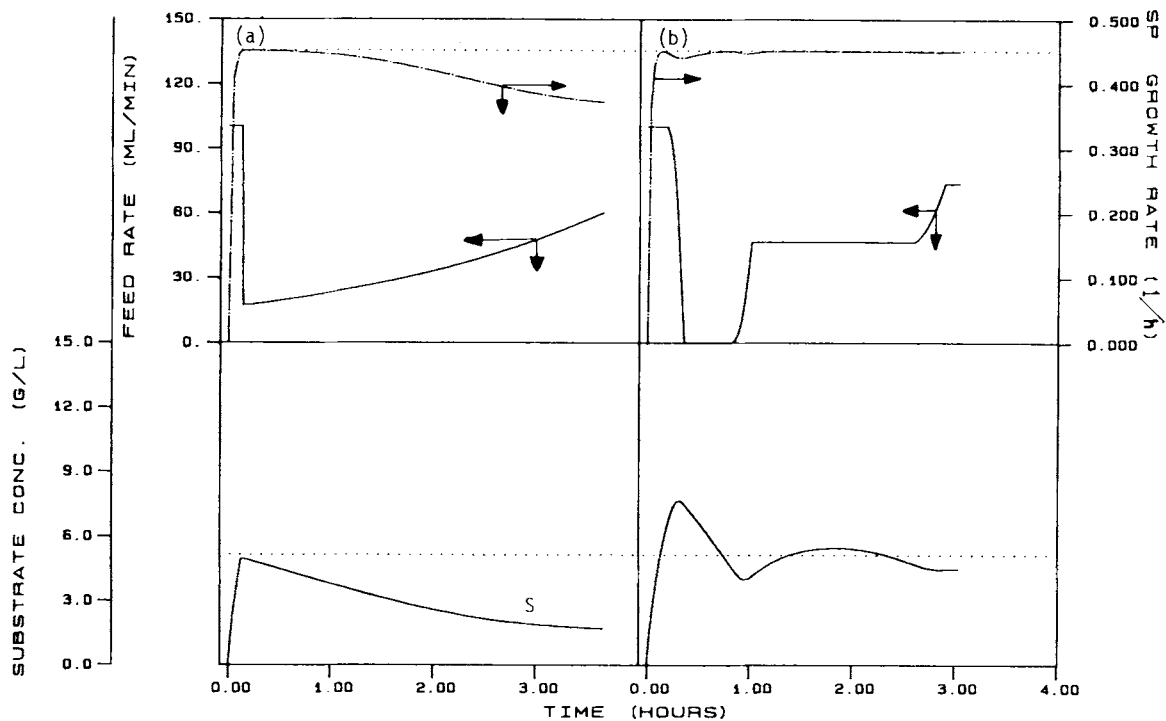


Figure 2. Specific growth rate (—) μ and (····) μ_{opt} , substrate concentration (—) S and (····) S_{opt} , and (—) feed-flow rate profiles for the case when μ_m is 25% higher than the model value (a) optimal open-loop solution based on Model 2 and (b) feedback controlled operation.

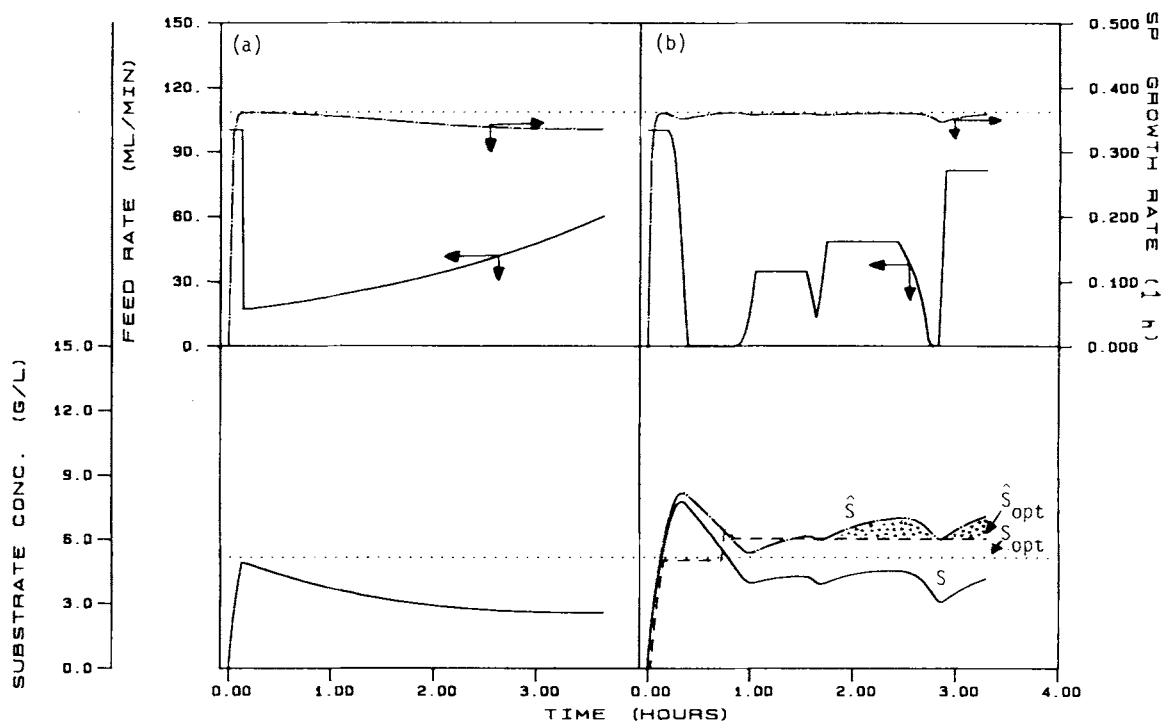


Figure 3. Specific growth rate (—) μ and (····) μ_{opt} , substrate concentration (—) S and (····) S_{opt} , and (—) feed-flow rate profiles for the case when $y_{X/S}$ is 25% lower than the actual model value (a) optimal open-loop solution based on Model 2 and (b) feedback controlled operation.

creasing the nutrient flow rate. Similarly the negative sign in eq. (5) applies to the case when $S > S_{opt}$. Therefore, with the knowledge of the position of S with respect to S_{opt} and estimates of μ and μ_{opt} , the control action described by

eq. (5) can be easily taken. It should be emphasized that the implementation of the control action does not require the exact on-line value of S , only the knowledge of the relative position of S with respect to S_{opt} is necessary.

To implement the above control algorithm, it is necessary to have an initial open-loop period of operation during which values of μ_{opt} and S_{opt} are identified. For simplicity, we first consider a case in which we have reliable on-line measurement or estimation of the substrate concentration. During the initial open-loop period, it is recommended that the nutrients be fed at the maximum possible rate which allows us to obtain good estimates of μ . In the present study, unless otherwise indicated, the initial feed rate was chosen to be 100 mL/min which corresponds to F/V_0 of 3.0 h^{-1} . The open-loop period continues until the μ values begin to decrease. The maximum value of μ obtained during this period is set as μ_{opt} and the corresponding value of S as S_{opt} . The control action described by eq. (5) is then initiated based on the current estimate of μ and S .

The μ_{opt} value identified by the controller during the initial open-loop period may not represent the true optimum value. This could be because the initial feed rate chosen may be so high as to bypass the S_{opt} value. Consequently, during the closed-loop operation, μ_{opt} and S_{opt} must be continually updated whenever the observed μ value is found to be greater than the μ_{opt} value. The proposed control scheme is schematically represented in Figure 4.

To evaluate the performance of the controller, a number of simulation studies were made. Figure 1(b) illustrates the performance of the control scheme for the case where the process follows the behavior described by Model 2 in Table I. After a brief initial period during which μ_{opt} and S_{opt} are identified, the controller does a very good job of controlling μ very close to μ_{opt} by exponentially increasing the feed-flow rate to maintain S near S_{opt} . The feed-flow rate

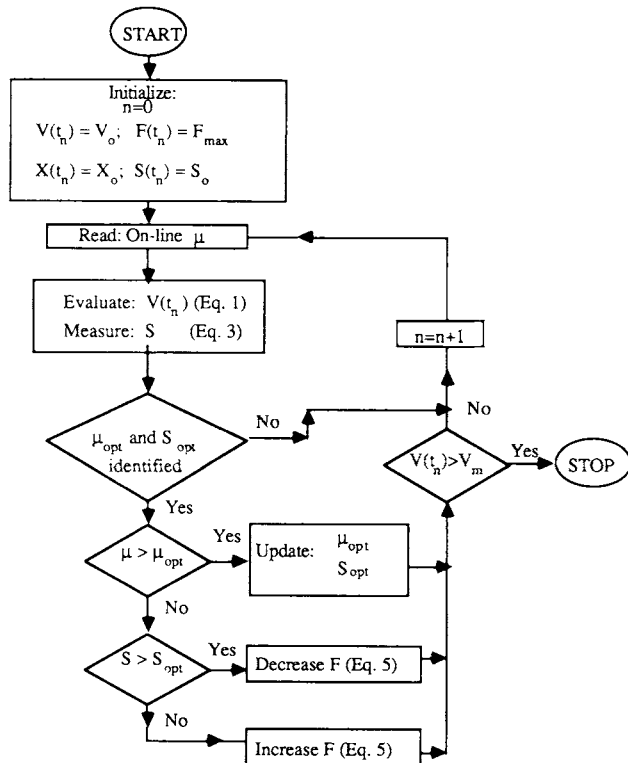


Figure 4. A flow diagram of the simple control algorithm.

under the closed-loop operation [Figure 1(b)] closely resembles the open-loop optimal feed schedule [Figure 1(a)] which was obtained using the maximum principle.

Figure 2 illustrates the applicability of the proposed algorithm to the case where the model parameter μ_m is 25% in error. Since the controller assumes no model, it simply identifies the correct μ_{opt} and S_{opt} values and manipulates the feed-flow rate to control μ at μ_{opt} . The controller successfully maintains the nutrient concentration in the fermentor near the optimal condition for growth (S_{opt}) [Figure 2(b)], whereas in the open-loop operation the nutrient concentration deviates considerably from the optimal value [Fig. 2(a)]. Consequently, the overall performance of the closed-loop operation is far superior to the performance of the open-loop operation in which the feed flow profile is based on an incorrect value of a parameter in the growth model.

In situations where it is difficult to obtain on-line measurement or estimates of S , it is proposed to estimate S as \hat{S} by integrating eqs. (1) and (3) with proper initial conditions, S_F , $y_{X/S}$ and on-line estimates of μ . An initial estimate of the optimal substrate concentration, \hat{S}_{opt} , can be obtained from \hat{S} values during the open-loop period in which, as discussed above, the μ_{opt} value is identified. The values of \hat{S} and \hat{S}_{opt} so obtained could both differ from true S and S_{opt} , respectively, due to errors involved in estimating the initial conditions, S_F , $y_{X/S}$, and μ . This could cause the proposed controller to take improper, nonoptimal action especially in cases which are illustrated in Figure 5. For example,

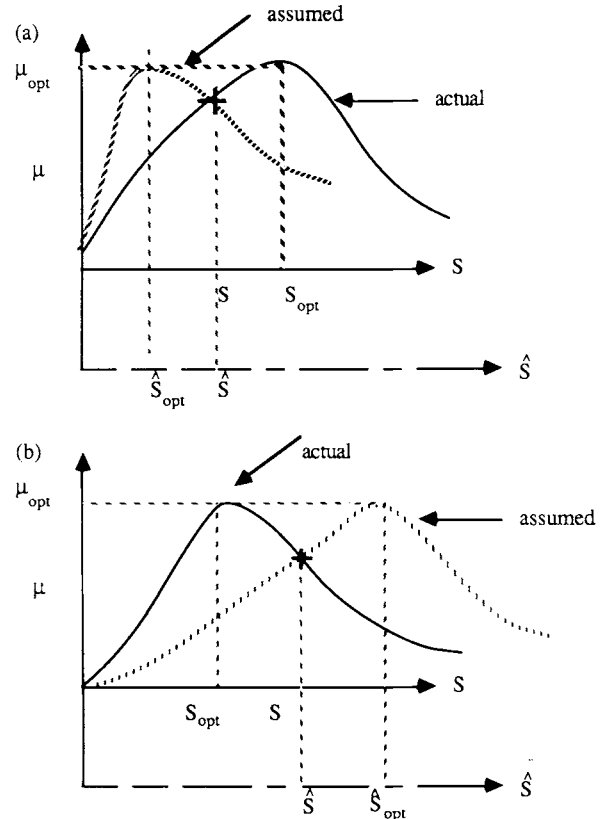


Figure 5. Profiles of specific growth rate with respect to substrate concentration (—) S and (·····) \hat{S} for case (a) $S < S_{\text{opt}}$ but $\hat{S} > \hat{S}_{\text{opt}}$ and (b) $S > S_{\text{opt}}$ but $\hat{S} \leq \hat{S}_{\text{opt}}$. Note “+” is the operating point and scales for S and \hat{S} could be different.

in Figure 5(a) the fermentor operating point (+) is such that $S < S_{opt}$ or $d\mu/dS > 0$ and therefore the controller should increase F_{in} to raise S to S_{opt} . However, due to incorrect estimates of S and S_{opt} the controller would infer $S > S_{opt}$, thereby taking improper control action by decreasing F_{in} . This improper control action would continue for a period in which F_{in} decreases sufficiently to cause \hat{S} to fall below \hat{S}_{opt} . Thereafter, the controller would correctly manipulate F_{in} to move S toward S_{opt} . An analogous situation is illustrated in Figure 5(b) where initially the controller would manipulate F_{in} in the wrong direction by increasing its value until the increase in F_{in} is sufficiently large to cause \hat{S} to rise above \hat{S}_{opt} . Once again, after an improper action the controller would manipulate F_{in} to take control action in the right direction. A combination of two factors: 1) large deviations in \hat{S} and \hat{S}_{opt} from S and S_{opt} , respectively, due to accumulated errors of integration; and 2) improper control action during periods when the relative position of S with respect to S_{opt} is inferred incorrectly, could force the operation of the fermentor in a suboptimal region for an extended portion of a fed-batch cycle. To eliminate this possibility, it is recommended that S_{opt} be updated periodically in the

proposed control scheme. This is achieved by stipulating that whenever μ enters a region close to μ_{opt} (e.g. $\pm 1\%$ of μ_{opt}) the \hat{S}_{opt} value be changed to the value of \hat{S} at that instant. Since \hat{S}_{opt} is to be updated during a closed-loop operation, we must ensure that any action taken to control μ does not interfere with the updating process. The foregoing requirement is met by specifying that no control action be taken as long as μ is moving toward the updating region ($\pm 1\%$ of μ_{opt}). A schematic of the final control algorithm is shown in Figure 6.

The results shown in Figure 3(b) are based on the control algorithm (Fig. 6) which has all the features discussed above. These results illustrate an interesting situation in which it is assumed that the model estimate of the cell-mass yield is in error, possibly due to a change in the culture condition. Since the actual cell-mass yield exhibited by the culture is 25% lower than the value used in eq. (3) to obtain \hat{S} , the \hat{S} values are consistently higher than the actual S values. Therefore, the identified \hat{S}_{opt} is higher than the actual S value. It should be noted that although the actual S_{opt} value remains constant, its estimate, \hat{S}_{opt} , changes during the fed-batch fermentation. The shaded portions

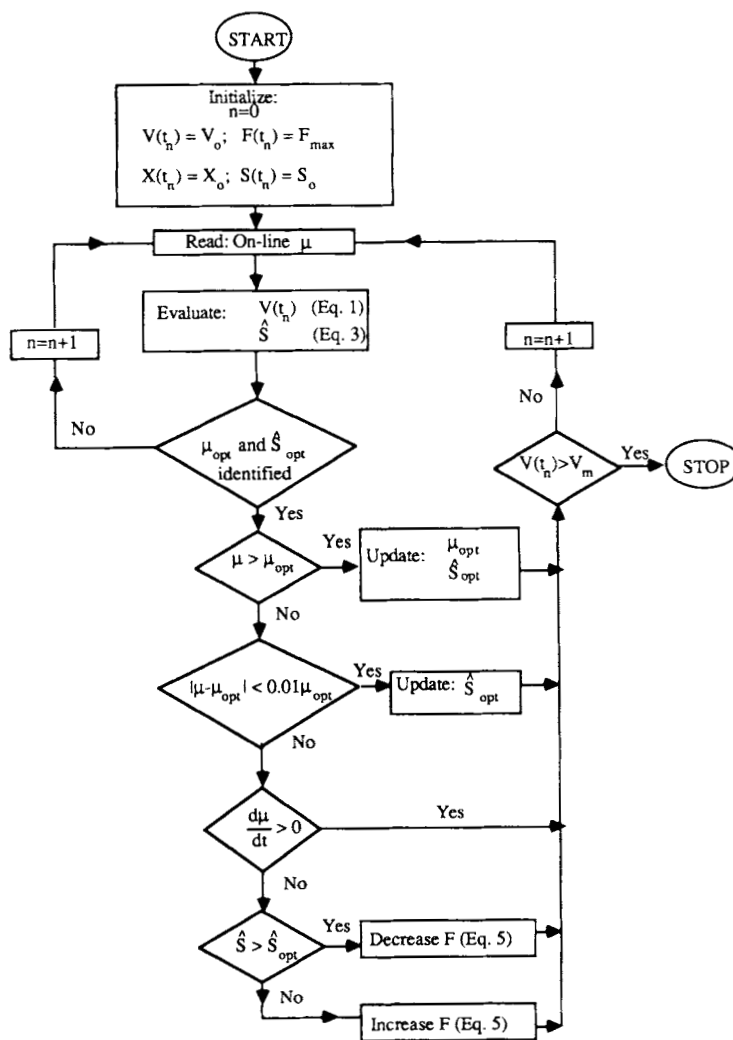


Figure 6. A flow diagram of the final control algorithm.

bounded by \hat{S} and \hat{S}_{opt} curves in Figure 3(b) indicate periods during which the relative position of S with respect to S_{opt} is incorrectly inferred by the controller and hence during such periods either the controller takes no action (if $d\mu/dS > 0$) or manipulates F_{in} in the incorrect direction. In spite of such undesirable periods of improper control action, the controlled operation [Fig. 3(b)] shows significant improvement over the uncontrolled operation [Fig. 3(a)] in which S and hence μ deviate significantly from their optimum values. This results in a longer fermentation time (3.65 h) in the uncontrolled operation as compared to the fermentation time (3.3 h) required in the controlled operation. The performance of the final control algorithm is now examined for a variety of situations commonly encountered in microbial fermentations.

Saturation-Kinetic Model

The control algorithm is evaluated for the case of a microbial system which exhibits saturation kinetics (Monod model) as described by Model 1 in Table I. The saturation-kinetic model does not exhibit any μ_{opt} ; the higher the substrate concentration rises, the higher the specific growth rate becomes. The controlled fed-batch fermentation results are shown in Figure 7(a). The results show that the controller maintains the feed at the initial maximum rate (F_{max}) till the final volume is reached. The closed-loop operation resembles the optimal open-loop solution for this case.¹ Clearly, the results illustrate the fact that this con-

troller would work well even if the microbial kinetics is such that it shows no optimum in μ with respect to the substrate concentration. This situation also arises in the case of a substrate inhibition model when the feed substrate concentration is lower than the optimum substrate concentration.

Continuous Fermentation

The control algorithm is tested for its ability to maintain μ at μ_{opt} in a constant volume continuous fermentor. The operation of a continuous fermentor at μ_{opt} without any feedback control is unstable and generally results in washout. As the profiles in Figure 7(b) show, the controller is able to control the specific growth rate in a continuous fermentor near μ_{opt} . As expected, the feed flow rate never settles to a steady value, but the average value is found to correspond to the optimum specific-growth rate value of 0.36 h^{-1} based on Model 2.

Variable-Yield Model

In many microbial fermentations the cell-mass yield is not necessarily a constant value. This could be due to maintenance or endogeneous metabolism requirements. Model 3 applies to the fermentation of methanol to single-cell protein by a methylotroph. This model¹² exhibits a decrease in $y_{X/S}$ at higher values for methanol as described by the yield function given in Table I. For this case, the results in Figure 8(a)

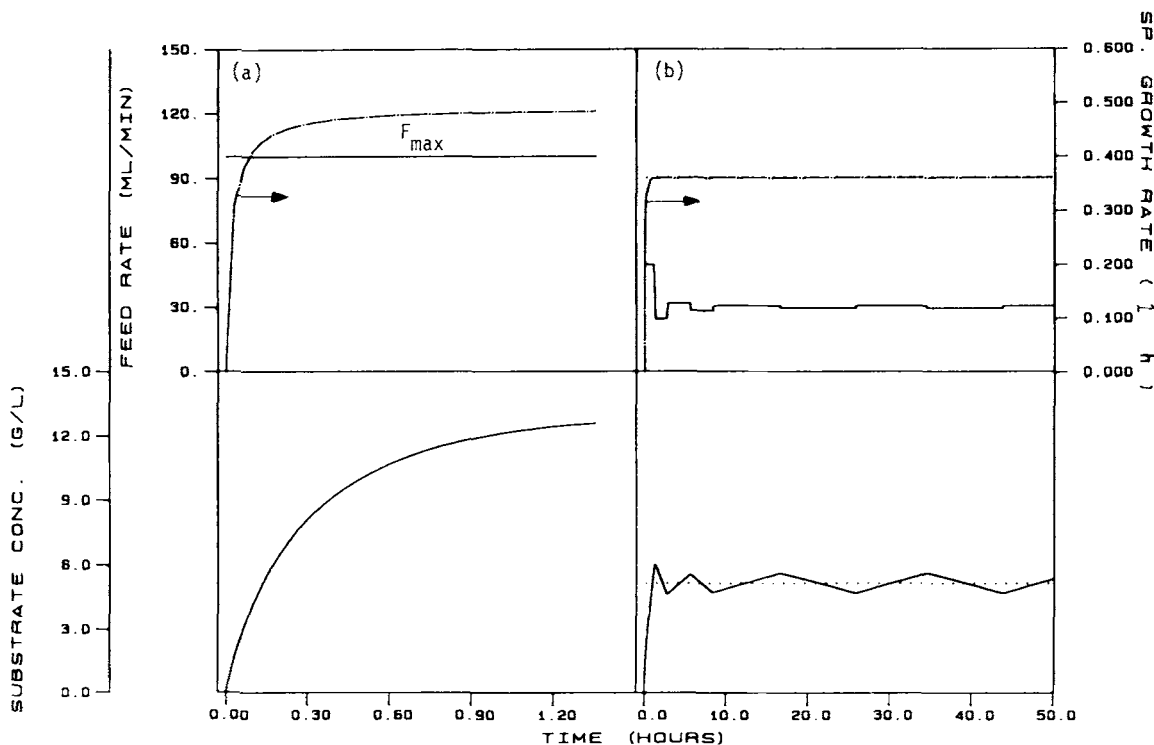


Figure 7. Specific growth rate (—) μ and (····) μ_{opt} , substrate concentration (—) S and (····) S_{opt} , and (—) feed-flow rate profiles under feedback controlled operations for (a) saturation-kinetic model (Model 1), and (b) continuous fermentor operation (Model 2).

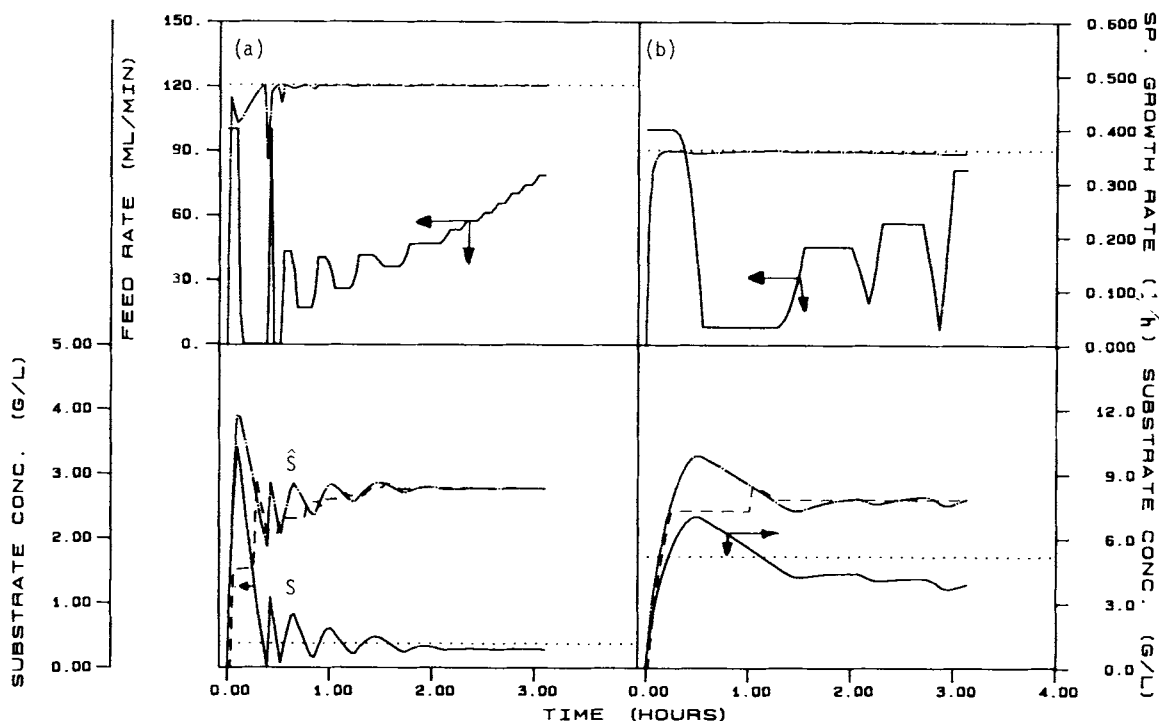


Figure 8. Specific growth rate (—) μ and (····) μ_{opt} ; substrate concentration (—) S ; (····) S_{opt} (—) \hat{S} ; and (····) \hat{S}_{opt} ; and (—) feed-flow rate profiles under feedback control for (a) variable yield model (Model 3) and (b) Model 2 based fed-batch controlled operation in which there is a 25% error in the feed substrate concentration S_F .

illustrate the performance of the control algorithm. Despite the fact that a constant $y_{X/S}$ value of 0.4 was assumed for estimating \hat{S} and \hat{S}_{opt} , the controller successfully controls μ at μ_{opt} during the course of fermentation.

Variation in Feed Substrate Concentration

Many microbial fermentation processes are based on natural but complex nutrient media (e.g., corn-steep liquor, vegetable oil, etc.). In such cases, it may be difficult to identify the exact value of the concentration of the limiting nutrient in the feed stream. Furthermore, the feed concentration of the limiting nutrient may change due to variations in the quality of the complex medium. Under these circumstances, a predetermined feed schedule may not result in optimal operation if the value of the feed concentration assumed is in error. The proposed algorithm can overcome this problem. This is illustrated by results in Figure 8(b) in which the actual value of the feed substrate concentration is 25% less than the assumed value. Consequently, \hat{S} and \hat{S}_{opt} values are higher than S and S_{opt} values, respectively. Nevertheless, continual updating of \hat{S}_{opt} , as discussed above, ensures operation of the fermentor at μ_{opt} .

Noise and Delay in Specific Growth Rate Estimation

Until now in our simulation study, it was assumed that exact and instantaneous values of μ are available for implementation of this control algorithm. In actual situations,

μ could be expected to be noisy and a time delay may be present in the estimate due to the method of estimation used or because of a delayed response of the culture to variations in substrate concentration. The independent impact of these factors on the performance of the proposed scheme was also examined in this study. Figure 9(a) shows the performance of this algorithm under noisy conditions. To simulate such a case, normally disturbed random noise of 5% amplitude and zero mean is added to μ values obtained using Model 2. Due to the noise in μ , the μ estimates were averaged over a 12-min interval to accurately track the overall path of μ . This simple modification is found sufficient to retain the effectiveness of the overall control algorithm.

A typical set of results illustrating the performance of the proposed algorithm under situations when noticeable time delays exist in estimates of μ is presented in Figure 9(b). It is assumed that each estimate of μ (based on Model 2) is delayed for purposes of feedback control action by eight minutes. A comparison of these results with the results presented in Figure 1(b), for cases where no time delay exist in estimation of μ , suggest that time delay in μ deteriorates the performance of control scheme by preventing it from maintaining μ near μ_{opt} as time progresses during a fed-batch fermentation. Nevertheless, a significant time delay of eight minutes in μ estimation results in only a modest decline in the overall cell mass productivity. Furthermore, it should be noted that a similar decline would occur in open-loop operation if the delay in μ is primarily due to a delay in the response of the culture due to changes in substrate concentration.

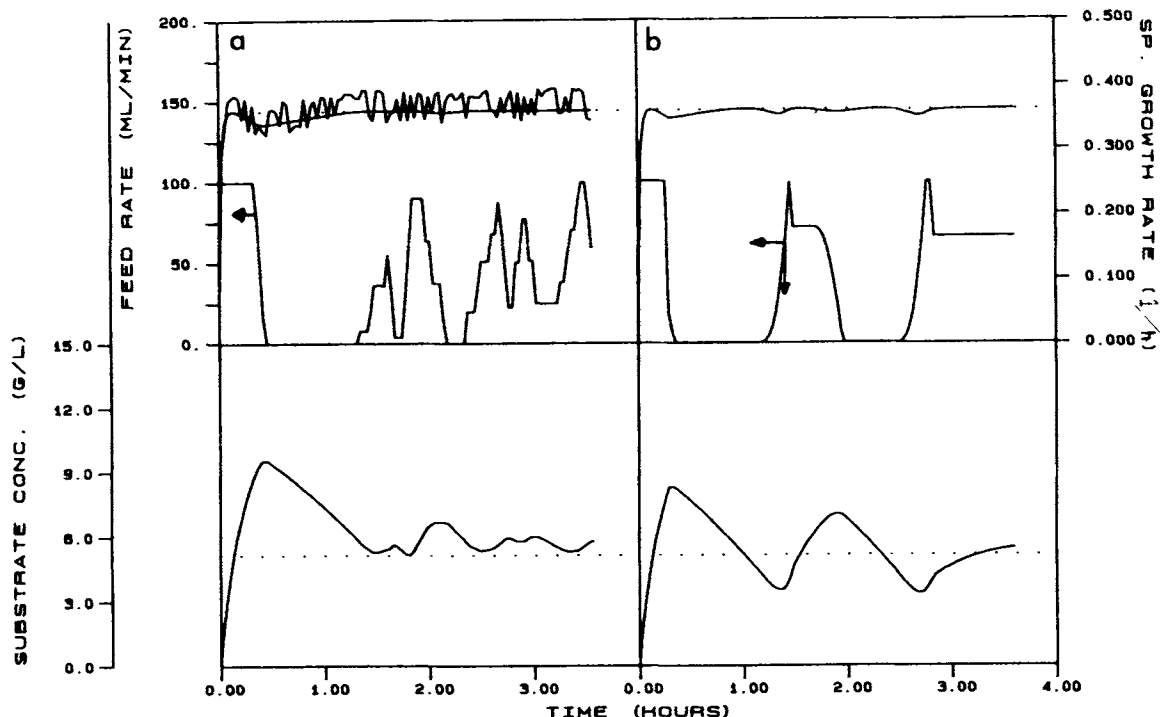


Figure 9. Specific growth rate (—) μ and (·····) μ_{opt} , substrate concentration (—) S and (·····) S_{opt} , and (—) feed-flow rate profiles. Model 2 based fed-batch controlled operation with (a) 5% zero-mean Gaussian noise in the estimated μ values and (b) eight minute time delay in μ estimate.

Product-Inhibited Fermentation

Many fermentations produce noncellular product (e.g., ethanol) that inhibit growth of microorganisms producing the product. Under such a situation, an optimum in μ with respect to the substrate concentration may decrease with time as the inhibitory product of fermentation accumulates in the culture medium. Model 4, a modified form of a model for whey fermentation,¹⁶ represents one such example. Application of the proposed control algorithm (Fig. 6) in such a case could result in undesirable controller performance due to the inability of the algorithm to track declining values of μ_{opt} . To overcome this problem, it is recommended that the control algorithm be forced to update μ_{opt} periodically by frequently setting μ_{opt} equal to the current value of μ . This modification of the proposed control algorithm is schematically illustrated in Figure 10. Here, M (an integer constant greater than 1) characterizes the μ_{opt} updating interval $M\Delta t$. The net effect of this is that after every $M\Delta t$ period μ_{opt} is set equal to μ which forces the algorithm to identify the current new value of μ_{opt} which is greater than or equal to the current observed value of μ . By forcing $\mu_{opt} = \mu$, this modification also prevents the controller from taking any control action until a new value of μ_{opt} different from the current value of μ is identified. Thus, too low a value of M is undesirable because it will force the algorithm to spend most of its time identifying μ_{opt} rather than controlling μ at μ_{opt} . Also, too high a value of M would prevent the algorithm from accurately tracking declining values of μ_{opt} . Consequently, M is a tuning parameter of the algorithm and it must be set appropriately depending on the fermentation kinetic at hand.

Figure 11 shows the performance of the modified control scheme as applied to the case of a culture whose behavior is described by Model 4. The model exhibits decrease in μ_{opt} with increase in product concentration in the culture. The simulation results are presented for two cases differing in terms of μ_{opt} updating intervals. In each case the algorithm is able to successfully maintain μ at declining μ_{opt} . However, use of a larger updating interval results in a feed profile which is too noisy and hence may be undesirable.

CONCLUSIONS

In this article, we have developed an algorithm for direct control of a fed-batch fermentor at the maximum possible specific growth rate. We have presented results of a detailed simulation study to demonstrate the effectiveness of this algorithm. The algorithm was primarily developed with the optimization of the cell-mass production in mind. However, it can be modified to optimize any other specific fermentation rate provided on-line estimates of that specific rate are available. For example, production of a secondary metabolite in a fed-batch fermentor can be optimized by changing the controlled variable to the specific metabolite production rate instead of the specific growth rate.

The algorithm does not require on-line measurements of substrate concentrations in the culture medium. It can be implemented based on the on-line estimate of the specific growth rate (μ) alone. It identifies the optimal condition for growth (\hat{S}_{opt} , μ_{opt}) on-line, continually updates these values, and manipulates the nutrient flow rate to control μ at μ_{opt} . A simple feedback law described by eq. (4) with controller

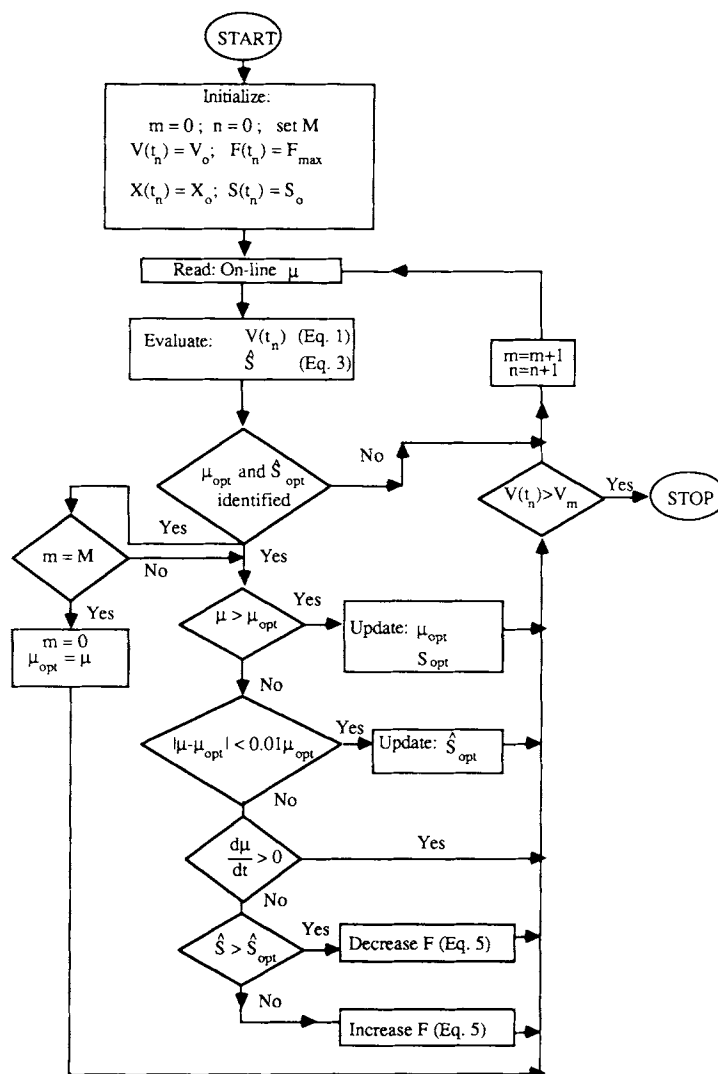


Figure 10. A flow diagram of the proposed control algorithm with a modification to account for a decrease in μ during the course of a fermentation.

constant $K_c = 12$ L was used in this simulation study. No attempt was made to optimize the control law or the controller constant. Moreover, our simulation results demonstrate that the algorithm could also handle situations where μ estimates are noisy or are in constant error with respect to the actual values.

The algorithm is model independent and therefore can be applied to many industrial fermentations which utilize crude, natural but complex nutrient media. For such purposes, it is generally difficult to develop a model that gives qualitative relationships between the fermentation state variables and the feed rate of the limiting nutrient. In such cases, a model-independent scheme seems to be the only solution for productivity optimization. The algorithm performs well even if no optimum value exists in the specific growth rate. Even though it was mainly developed to control μ at its optimum value in a fed-batch fermentor, it performs this task well in a continuous fermentor as well.

The control methodology proposed here should work well even under situations when the microbial system undergoes

adaptation. This could be manifested in terms of change in optimum values of substrate concentration and specific growth rate as well as a change in the cell-mass yield.

NOMENCLATURE

a	constant in Model 3 (g/L) ⁻¹
b	constant in Model 3 (g/L) ⁻¹
c	constant in Model 3 (g/L) ⁻²
F	flow rate of medium (L/h)
K_c	control constant (L)
K_i	inhibition constant (g/L)
K_m	saturation constant (g/L)
S	substrate concentration (g/L)
\hat{S}	estimated substrate concentration (g/L)
t	time (h)
V	fermentor volume (L)
X	cell-mass concentration (g/L)
$y_{x/s}$	cell-mass yield (g/g)

Greek letters

μ	specific growth rate (h ⁻¹)
μ_m	maximum specific growth rate (h ⁻¹)

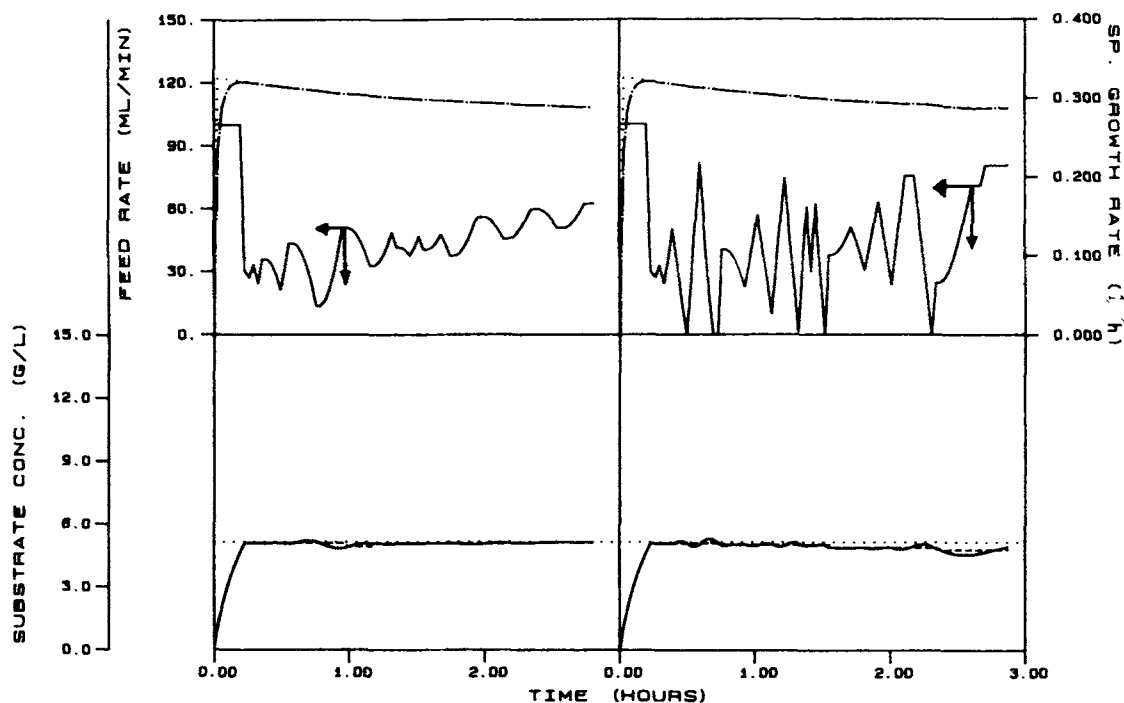


Figure 11. Specific growth rate (—) μ and (····) μ_{opt} ; substrate concentration (—) S , (····) S_{opt} ; and (—) \dot{S}_{opt} ; and (—) feed-flow rate profiles under feedback control for Model 4 with μ_{opt} updated every (a) 12 min and (b) 48 min.

Subscripts

F feed condition
 opt optimum condition

This work was supported in part by a grant from the National Science Foundation, No. CPE-8404623.

References

1. W. A. Weigand, *Biotechnol. Bioeng.*, **23**, 249 (1981).
2. B. E. Stutts, H. C. Lim, and W. A. Weigand, unpublished.
3. P. J. Hennigan, M. J. Rolf, W. A. Weigand, and H. C. Lim, in *Computer Applications in Fermentation Technology* (Society of Chemical Industry, London, 1982), p. 99.
4. M. J. Rolf, P. J. Hennigan, R. D. Mohler, W. A. Weigand, and H. C. Lim, *Biotechnol. Bioeng.*, **24**, 1191 (1982).
5. A. Constantinides, *Ann. NY Acad. Sci.*, **326**, 193 (1979).
6. T. Yamane and S. Shimizu, in *Advances in Biochemical Engineering/Biotechnology*, A. Fiechter, Ed. (Springer-Verlag, New York), Vol. 30, pp. 145–194.
7. S. Parulekar and H. C. Lim, in *Advances in Biochemical Engineering/Biotechnology*, A. Fiechter, Ed. (Springer-Verlag, New York), Vol. 32, pp. 207–258.
8. G. D'Ans, D. Gottlieb, and P. Kokotovic, *Automatica*, **8**, 729 (1972).
9. T. Yamane, T. Kume, E. Dada, and T. Takamatsu, *J. Ferment. Technol.*, **55**, 587 (1977).
10. J. Staniskis and D. Levisauskas, *Biotechnol. Bioeng.*, **26**, 419 (1984).
11. V. M. Edwards, *Biotechnol. Bioeng.*, **12**, 679 (1970).
12. D. DiBiasio, H. C. Lim, and W. A. Weigand, *AIChE J.*, **27**, 284 (1981).
13. W. Wu, K. Chen, and H. Chiou, *Biotechnol. Bioeng.*, **27**, 756 (1985).
14. S. H. Park, K. T. Hong, J. H. Lee, and J. H. Bae, *Env. J. Appl. Microbiol. Biotechnol.*, **17**, 68 (1983).
15. K. San and G. Stephanopoulos, *Biotechnol. Bioeng.*, **26**, 1209 (1984).
16. J. E. Bailey and D. F. Ollis, *Biochemical Engineering Fundamentals*, 2nd ed. (McGraw-Hill, New York, 1986).